

MIMO Intensity-Modulation Channels: Capacity Bounds and High SNR Characterization

Anas Chaaban, Zouheir Rezki, and Mohamed-Slim Alouini

Abstract—The capacity of MIMO intensity modulation channels is studied. The nonnegativity of the transmit signal (intensity) poses a challenge on the precoding of the transmit signal, which limits the applicability of classical schemes in this type of channels. To resolve this issue, capacity lower bounds are developed by using precoding-free schemes. This is achieved by channel inversion or QR decomposition to convert the MIMO channel to a set of parallel channels. The achievable rate of a DC-offset SVD based scheme is also derived as a benchmark. Then, a capacity upper bound is derived and is shown to coincide with the achievable rate of the QR decomposition based scheme at high SNR, consequently characterizing the high-SNR capacity of the channel. The high-SNR gap between capacity and the achievable rates of the channel inversion and the DC-offset SVD based schemes is also characterized. Finally, the ergodic capacity of the channel is also briefly discussed.

I. INTRODUCTION

Intensity-modulation is a simple transmission technique which uses the signal intensity to transmit information from a source to a destination. Its practical simplicity is appealing especially when it comes to optical-wireless communications (OWC), where it is considered an effective low-complexity/cost technique. In this context, the information bearing signal is the optical intensity, and the receiver employs a photo-diode for detection.

This intensity-modulation direct-detection (IM-DD) scheme has attracted increasing research interest recently due to the revival of OWC [1], and the increasing interest in visible-light communication (VLC) [2]. Many aspects of OWC has been studied recently, for both outdoors and indoors applications. One such aspect is multi-aperture OWC, where multiple light sources are used at the transmitter and/or multiple detectors are used at the receiver, which forms a multi-input multi-output (MIMO) system. For example, the utility of MIMO in fading channels has been explored in [3], [4], the performance of the V-BLAST architecture in MIMO OWC was studied in [5], [6], and transmission techniques and channel models for indoors MIMO OWC have been investigated in [7], [8]. These works mostly focus on error rate and outage performance.

Another equally important performance metric is the channel capacity, which specifies the highest rate of reliable information transmission over a channel. Although the capacity of MIMO OWC modeled as a MIMO Poisson channel was studied in [9], [10], the capacity of the Gaussian IM-DD model

was not, to the best of our knowledge. The Gaussian IM-DD channel is an additive channel with independent Gaussian noise, and models OWC when electrical and background noises dominate the signal dependent noise. The main difference between MIMO IM-DD Gaussian channels and radio-frequency (RF) Gaussian channels is in the input constraints, manifested in non-negativity and average constraints in OWC as opposed to power constraints in RF.

Due to this main difference, the elegant singular-value decomposition (SVD) scheme used to transform RF MIMO channels to parallel channels is not directly applicable in MIMO IM-DD channels. The reason is that precoding using the right singular vectors of the IM-DD channel matrix might lead to negative signals. This complication can be overcome by applying a DC offset [11], [12], conveniently leading to a positive signal, although simultaneously imposing a constraint on the codeword symbols. This restriction can be avoided by refraining from precoding at the transmitter and relying on post-coding at the receiver instead. Examples are channel inversion [7] and QR decomposition [13].

In this paper, we study the capacity of MIMO IM-DD Gaussian channels with a total average optical intensity constraint. This can model VLC systems with multiple light fixtures and multiple detectors [8] with a constraint on the total light intensity due to lighting requirements e.g., or an RGB (red/green/blue) color-shift keying system [14]. We first derive the achievable rates of channel inversion, QR decomposition, and DC-offset SVD based schemes. Then, to assess the performance of those schemes, we derive a capacity upper bound.

As intuition suggests, QR decomposition outperforms channel inversion, since the latter amplifies noise. It also outperforms the DC-offset SVD based scheme. We further show that a combination of QR decomposition, equal intensity allocation, and an exponential input distribution achieves the capacity of the channel at high SNR, thus characterizing the high SNR asymptotic capacity of the channel. Then, we derive the high-SNR capacity-gap of the channel inversion and the DC-offset SVD based schemes, for which we show that this gap is always positive. In the absence of channel-state information (CSI) at the transmitter, and under an equal intensity allocation constraint, we also demonstrate numerically that the QR decomposition based scheme achieves the ergodic capacity of the channel.

II. MODEL

Consider an OWC system comprising N transmit and N receive apertures, employing IM-DD. Denote the light intensity

A. Chaaban and M.-S. Alouini are with the Division of Computer, Electrical, and Mathematical Sciences and Engineering (CEMSE) at King Abdullah University of Science and Technology (KAUST), Thuwal, Saudi Arabia. Email: {anas.chaaban, slim.alouini}@kaust.edu.sa.

Z. Rezki is with the Department of Electrical and Computer Engineering, University of Idaho, Moscow, ID, USA. Email: zrezki@uidaho.edu.

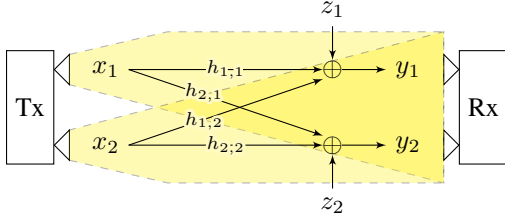


Fig. 1: An optical wireless communication system with two transmit apertures and two detectors: $x_i \geq 0$ is the optical intensity, $h_{i,j} \geq 0$ is a channel gain, and z_i is Gaussian noise.

of the i th transmitter by x_i , and the received signal at the j th receiver by y_j . The received vector $\mathbf{y} = (y_1, \dots, y_N)^T$ can be expressed in terms of the input vector $\mathbf{x} = (x_1, \dots, x_N)^T$ as (Fig. 1)

$$\mathbf{y} = \mathbf{H}\mathbf{x} + \mathbf{z}, \quad (1)$$

$\mathbf{z} = (z_1, \dots, z_N)^T$ is a vector of independent Gaussian noises with zero mean and unit variance ($\mathcal{N}(0, 1)$),¹ and $\mathbf{H} \in \mathbb{R}_+^{N \times N}$ is a matrix with elements $h_{j,i} \geq 0$ being the channel gain from transmitter i to receiver j . We assume that \mathbf{H} is invertible; see e.g. [8], [14].²

The transmit signal x_i is a realization of a random variable X_i which satisfies

$$X_i \geq 0, \text{ and } \sum_{i=1}^N \underbrace{\mathbb{E}[X_i]}_{\mathcal{E}_i} \leq \mathcal{E}. \quad (2)$$

The latter constraint is a total optical intensity constraint, such as a lighting constraint in a VLC system.³ We denote the vector of average intensities $(\mathcal{E}_1, \dots, \mathcal{E}_N)$ by \mathcal{E} .

We are interested in the capacity $C(\mathbf{H}, \mathcal{E})$ of this channel, defined as the highest achievable rate R that can be guaranteed with vanishing probability of error. Throughout the paper, we assume the availability of CSI at the receiver. The availability/quality of CSI at the transmitter depends on the regime of operation and is to be discussed later.

III. PRELIMINARIES

The results we present on the capacity of this MIMO system are expressed in terms of the capacity of a SISO system [15]–[17]. Consider a SISO channel with input x satisfying $\mathbb{E}[X] \leq \mathcal{E}$ and output $y = hx + z$ where z is $\mathcal{N}(0, 1)$ and $h \in \mathbb{R}_+$. We denote the capacity of this channel by $c(h, \mathcal{E})$, and lower and upper bounds on this capacity by $r(h, \mathcal{E})$ and $\bar{r}(h, \mathcal{E})$, respectively. We use a subscript to distinguish between different lower bounds. We give some examples next, which will be used in the sequel.

An achievable rate in this channel is given by

$$r_e(h, \mathcal{E}) = \frac{1}{2} \log \left(1 + \frac{eh^2\mathcal{E}^2}{2\pi} \right), \quad (3)$$

¹Input-independent Gaussian noise model [15].

²Note that if \mathbf{H} is not invertible, one can always ignore dependent columns to obtain an invertible reduced channel matrix.

³This is in contrast with the RF Gaussian MIMO channel where $X_i, h_{j,i} \in \mathbb{C}$ and $\sum_{i=1}^N \mathbb{E}[|X_i|^2] \leq P$.

achieved using an exponentially distributed X [15]. Another achievable rate has been given in [16] as

$$r_g(h, \mathcal{E}) = \max_{\ell > 0} I(X; Y) \quad (4)$$

where X follows a Geometric distribution $P(x) = \sum_{k=0}^{\infty} p(1-p)^k \delta(x - k\ell)$ where $p = \frac{\ell}{\ell + \mathcal{E}}$.

In practice, one is often interested in using a DC-offset input $x = s + t$ where $t = \mathcal{E}$ and $-\mathcal{E} \leq s \leq \mathcal{E}$ with $\mathbb{E}[S] = 0$. Practical schemes such as on-off keying and M -PAM (pulse-amplitude modulation) fall under this category. This leads to a peak-constrained input (peak $2\mathcal{E}$) for which the following rate is achievable

$$r_u(h, \mathcal{E}) = \frac{1}{2} \log \left(1 + \frac{2h^2\mathcal{E}^2}{\pi e} \right), \quad (5)$$

using a uniformly distributed (continuous) X [15].⁴ Note that this lower bound is smaller than $r_e(h, \mathcal{E})$. Nevertheless, it is useful for DC-offset schemes as we shall see later. One could also use a discrete uniform distribution (M -PAM) instead of a continuous one. The achievable rate in this case can be written as

$$r_p(h, \mathcal{E}) = \max_{M > 1} I(X; Y), \quad (6)$$

where $X = \mathcal{E} + S$ and S follows a uniform distribution on the M -ary alphabet $\{-\mathcal{E} + i \frac{2\mathcal{E}}{M-1} | i = 0, \dots, M-1\}$.

Thus, capacity is lower bounded by

$$c(h, \mathcal{E}) \geq r_m(h, \mathcal{E}), \quad m \in \{e, g, u, p\}. \quad (7)$$

We will restrict our attention to these lower bounds henceforth.

A capacity upper bound has been given in [15] as

$$c(h, \mathcal{E}) \leq \bar{r}(h, \mathcal{E}) = \inf_{\beta, \delta > 0} b(h, \mathcal{E}, \beta, \delta), \quad (8)$$

where $b(h, \mathcal{E}, \beta, \delta)$ is given in (9) at the top of the next page. We will also restrict our attention to this bound since it is fairly tight, especially at high SNR.

Next, we focus on the MIMO channel, and study its capacity in terms of the aforementioned bounds.

IV. ACHIEVABLE RATES

Precoding and post-coding are commonly used in MIMO transmission schemes. In RF MIMO channels, SVD can be used to design optimal precoders and postcoders. In our case, the nonnegativity constraint of \mathbf{x} poses a challenge against using this procedure. Namely, if the information bearing symbols are represented by $\mathbf{s} \in \mathbb{R}^N$ and the transmit precoder is \mathbf{V} (i.e., $\mathbf{U}\Sigma\mathbf{V}^T$ is the SVD of \mathbf{H}), then $\mathbf{V}\mathbf{s} \in \mathbb{R}_+^N$ must be satisfied for any \mathbf{s} , posing an additional constraint on its alphabet (cf. [12]). To alleviate this restriction, one can either refrain from precoding and rely on post-coding at receiver side, or apply a DC-offset SVD scheme.

⁴The achievable rates $r_e(h, \mathcal{E})$ and $r_u(h, \mathcal{E})$ are in fact lower bounds on the rates that can be achieved using an exponential and a uniform input distribution, respectively [15].

$$b(h, \mathcal{E}, \beta, \delta) = \log \left(\frac{\beta e^{-\frac{\delta^2}{2}}}{\sqrt{2\pi e}} + \frac{\mathcal{Q}(\delta)}{\sqrt{e}} \right) + \frac{\mathcal{Q}(\delta)}{2} + \frac{\delta^2}{2} - \frac{\mathcal{Q}(\delta + h\mathcal{E})}{2} + \frac{\delta + h\mathcal{E}}{\beta} + \frac{e^{-\frac{\delta^2}{2}}}{\sqrt{2\pi}} \left(\frac{1}{\beta} + \frac{\delta}{2} \right). \quad (9)$$

A. Precoding Free Schemes

The advantage of these schemes is that they retain the flexibility in choosing \mathbf{s} , and also leads to less CSI requirements at the transmitter. Motivated by this, we use $\mathbf{x} = \mathbf{s}$, where s_i , $i \in \{1, \dots, N\}$, is a symbol of a codeword $s_i^{[n]} = (s_i(1), \dots, s_i(n))$, the t th symbol of which is transmitted in time instant t . To decode the N transmitted streams $s_i^{[n]}$, $i \in \{1, \dots, N\}$, the receiver uses post-coding by either channel inversion or QR decomposition to transform the channel into a set of parallel SISO channels.

1) *Channel-Inversion Receiver*: In a channel-inversion receiver, the received signal is multiplied by $\mathbf{U} = \mathbf{H}^{-1}$ to obtain a set of parallel channels. The following statement provides an achievable rate using this receiver.

Proposition 1: An achievable rate using channel inversion is given by

$$R_m^{[I]}(\mathbf{H}, \mathcal{E}) = \max_{\mathcal{E} \in \mathcal{S}} \sum_{i=1}^N r_m(\|\mathbf{u}_i\|^{-1}, \mathcal{E}_i), \quad (10)$$

where $m \in \{\mathbf{e}, \mathbf{g}\}$,⁵ \mathbf{u}_i^T is the i th row of $\mathbf{U} = \mathbf{H}^{-1}$, and

$$\mathcal{S} = \{\mathcal{E} \in \mathbb{R}_+^N \mid \mathcal{E}_1 + \dots + \mathcal{E}_N \leq \mathcal{E}\}. \quad (11)$$

Proof: Multiplying \mathbf{y} by \mathbf{U} yields $\bar{\mathbf{y}} = \mathbf{x} + \mathbf{U}\mathbf{z} = \mathbf{x} + \bar{\mathbf{z}}$. This leads to a set of parallel channels with correlated noises since $\mathbb{E}[\bar{\mathbf{z}}\bar{\mathbf{z}}^T] = \mathbf{U}\mathbf{U}^T$. As a simple treatment, the receiver ignores this correlation and decodes each x_i from $\bar{y}_i = x_i + \bar{z}_i$, where \bar{z}_i is $\mathcal{N}(0, \|\mathbf{u}_i\|^2)$, and \mathbf{u}_i^T is the i th row of \mathbf{U} . This is equivalent to a SISO channel with channel gain $\|\mathbf{u}_i\|^{-1}$ and unit noise variance whose capacity is $c(\|\mathbf{u}_i\|^{-1}, \mathcal{E}_i)$, where \mathcal{E}_i is the average intensity allocated to this channel. Using the capacity lower bound (7), and maximizing with respect to \mathcal{E} concludes the proof. ■

Under an exponential input distribution ($m = \mathbf{e}$ in (10)), the optimal intensity allocation \mathcal{E} satisfies

$$\mathcal{E}_i = \frac{1}{2\lambda} \pm \sqrt{\frac{1}{4\lambda^2} - \frac{1}{c_i^2}} \quad (12)$$

where $c_i = \|\mathbf{u}_i\|^{-1} \sqrt{\frac{e}{2\pi}}$, and $\lambda > 0$ is chosen so that $\sum_{i=1}^N \mathcal{E}_i = \mathcal{E}$, and a reliable approximate solution can be obtained using the simple algorithm in [18]. This allocation can also be used for $m = \mathbf{g}$. The achievable rate in (10) can be improved by exploiting the noise correlation to reduce the noise variance in a successive manner. That is, after decoding (x_1, \dots, x_{i-1}) , \bar{z}_i is estimated from $(\bar{y}_1, \dots, \bar{y}_i)$ given (x_1, \dots, x_{i-1}) , the estimate is subtracted from \bar{y}_i , and then x_i is decoded. Another way to improve this achievable rate is using the QR decomposition as described next.

2) *QR-Decomposition Receiver*: In this case, the receiver employs a QR-decomposition to reduce the channel into a more desirable structure, where successive decoding of the N streams can be easily applied. Let the QR decomposition of \mathbf{H} be

$$\mathbf{H} = \mathbf{Q}\mathbf{R}, \quad (13)$$

where \mathbf{Q} is orthogonal and \mathbf{R} is upper triangular. An achievable rate using this scheme is given next.

Proposition 2: An achievable rate using a QR-decomposition receiver is given by

$$R_m^{[QR]}(\mathbf{H}, \mathcal{E}) = \max_{\mathcal{E} \in \mathcal{S}} \sum_{i=1}^N r_m(|r_{i,i}|, \mathcal{E}_i), \quad (14)$$

where $m \in \{\mathbf{e}, \mathbf{g}\}$, $r_{i,i}$ is the (i, i) component of \mathbf{R} defined in (13), and \mathcal{S} is defined in (11).

Proof: The received signal can be written as $\mathbf{y} = \mathbf{Q}\mathbf{R}\mathbf{x} + \mathbf{z}$. The receiver multiplies \mathbf{y} by \mathbf{Q}^T to obtain

$$\tilde{\mathbf{y}} = \mathbf{R}\mathbf{x} + \tilde{\mathbf{z}}, \quad (15)$$

where $\tilde{\mathbf{z}} = \mathbf{Q}\mathbf{z}$, whose components are independent $\mathcal{N}(0, 1)$. The receiver starts by decoding x_N from $\tilde{y}_N = r_{N,N}x_N + \tilde{z}_N$. This can be done reliably if the rate of the N th stream is below the capacity of this channel, $c(|r_{N,N}|, \mathcal{E}_N)$, where \mathcal{E}_N is the average intensity of x_N . The receiver then subtracts the contribution of x_N from \tilde{y}_{N-1} and decodes x_{N-1} , which can be done reliably if the rate of stream $N-1$ is below $c(|r_{N-1,N-1}|, \mathcal{E}_{N-1})$. This proceeds until all N streams have been decoded. Using the capacity lower bound (7) and optimizing with respect to \mathcal{E} leads to the desired result. ■

The allocation in (12) can be used here as well.

B. DC-offset SVD

In this case, SVD precoding is applied at the transmitter, and a DC offset is applied to guarantee the nonnegativity of the transmit signal. Let the SVD of \mathbf{H} be written as

$$\mathbf{H} = \mathbf{U}\mathbf{\Sigma}\mathbf{V}^T, \quad (16)$$

where \mathbf{U} and \mathbf{V} are orthogonal $N \times N$ matrices and $\mathbf{\Sigma}$ is a diagonal $N \times N$ matrix. The transmit signal is constructed as $\mathbf{x} = \mathbf{V}\mathbf{s} + \mathbf{t}$, where \mathbf{t} is a DC offset and s_i is a symbol of the codeword $s_i^{[n]}$ satisfying $-a_i \leq s_i \leq a_i$ and $\mathbb{E}[S_i] = 0$. An achievable rate using this scheme is given next.

Proposition 3: An achievable rate using a DC-offset SVD transmission scheme is given by

$$R_m^{[SVD]}(\mathbf{H}, \mathcal{E}) = \max_{\mathbf{a} \in \mathcal{T}} \sum_{i=1}^N r_m(\sigma_i, a_i), \quad (17)$$

⁵We exclude $r_u(h, \mathcal{E})$ here because it is smaller than $r_e(h, \mathcal{E})$.

where $m \in \{u, p\}$, σ_i is the (i, i) component of Σ defined in (16), and \mathcal{T} is defined as

$$\mathcal{T} = \left\{ \mathbf{a} \in \mathbb{R}_+^N \left| \sum_{i=1}^N \sum_{j=1}^N |v_{i,j}| a_j \leq \varepsilon \right. \right\}, \quad (18)$$

with $v_{i,j}$ being the (i, j) component of \mathbf{V} .

Proof: Let the average optical intensity of aperture i be \mathcal{E}_i . Since $\mathbb{E}[S_i] = 0$, then $\mathbb{E}[X_i] = t_i$ and hence $t_i = \mathcal{E}_i$. To guarantee nonnegativity, it is required that $\mathcal{E}_i = \sum_{j=1}^N |v_{i,j}| a_j$. Upon receiving $\mathbf{y} = \mathbf{H}\mathbf{x} + \mathbf{z}$, the receiver subtracts $\mathbf{H}\mathbf{t}$ and multiplies the result by \mathbf{U}^T to obtain $\hat{\mathbf{y}} = \Sigma\mathbf{s} + \hat{\mathbf{z}}$ where $\hat{\mathbf{z}}$ is a vector of independent $\mathcal{N}(0, 1)$ noises. This is a parallel channel where $\hat{y}_i = \sigma_i s_i + \hat{z}_i$. The achievable rate over channel i is $r_u(\sigma_i, a_i)$ using a continuous uniform input distribution (5), or $r_p(\sigma_i, a_i)$ using a discrete uniform input distribution (6). Thus, the overall achievable rate is given by $\sum_{i=1}^N r_m(\sigma_i, a_i)$, $m \in \{u, p\}$, which is to be maximized with respect to a_i subject to $\sum_{i=1}^N \sum_{j=1}^N |v_{i,j}| a_j \leq \varepsilon$. This concludes the proof. ■

Note that this scheme requires bounded s_i so that a DC-offset suffices to make $x_i \geq 0$. Thus, the only possible input in this case is one that satisfies $s_i \in [-a_i, a_i]$ for some $a_i > 0$, and hence the restriction to $r_u(h, \mathcal{E})$ and $r_p(h, \mathcal{E})$.

The main difference between the maximizations in $R^{[SVD]}(\mathbf{H}, \mathcal{E})$ and $R^{[QR]}(\mathbf{H}, \mathcal{E})$ is the feasible set \mathcal{T} which is different from \mathcal{S} . The optimal allocation of a_i for $m = u$ in this case can be obtained similar to [18], and is given by

$$a_i = \frac{1}{2\lambda\nu_i} \pm \sqrt{\frac{1}{4\lambda^2\nu_i^2} - \frac{1}{c_i^2}} \quad (19)$$

where $\nu_i = \sum_{j=1}^N |v_{j,i}|$, $c_i = \sigma_i \sqrt{\frac{2}{\pi e}}$, and $\lambda > 0$ is chosen so that $\sum_{i=1}^N a_i \nu_i = \varepsilon$. An algorithm similar to the one in [18] (with minor modifications) can be used for finding a reliable solution. This allocation can be also used for $m = p$.

To assess the performance of these three schemes, we develop a capacity upper bound next.

V. CAPACITY UPPER BOUND

To derive a capacity upper bound, we also rely on the QR decomposition of the channel. The upper bound is given next.

Theorem 1: The capacity of a MIMO IM-DD channel with an invertible channel matrix \mathbf{H} with QR-decomposition $\mathbf{Q}\mathbf{R}$ is upper bounded by

$$\bar{C}(\mathbf{H}, \mathcal{E}) = \max_{\mathcal{E} \in \mathcal{S}} \sum_{i=1}^N \bar{r}(s_{i,i}^{-\frac{1}{2}}, \mathcal{E}_i) + \frac{1}{2} \log \left(\frac{\prod_{i=1}^N s_{i,i}}{|\mathbf{S}|} \right),$$

where $\mathbf{S} = \mathbf{R}^{-1}\mathbf{R}^{-T}$, $s_{i,i}$ its (i, i) component, and $\bar{r}(\cdot, \cdot)$ is as given in (8).

Proof: Since the orthogonal transformation \mathbf{Q} is invertible, the transformed channel (15) has the same capacity as the original channel. Denoting the random variables representing \mathbf{x} and $\hat{\mathbf{y}}$ by \mathbf{X} and $\tilde{\mathbf{Y}}$, this capacity can be written as

$$C = \max_{p(\mathbf{x})} I(\mathbf{X}; \tilde{\mathbf{Y}}) = \max_{p(\mathbf{x})} I(\mathbf{X}; \tilde{\mathbf{Y}}'), \quad (20)$$

where $p(\mathbf{x})$ is the distribution of $\mathbf{X} \in \mathbb{R}_+^N$ satisfying $\sum_{i=1}^N \mathbb{E}[X_i] \leq \varepsilon$, $\tilde{\mathbf{Y}}' = \mathbf{R}^{-1}\tilde{\mathbf{Y}} = \mathbf{X} + \tilde{\mathbf{Z}}'$, and $\tilde{\mathbf{Z}}' = (\tilde{Z}'_1, \dots, \tilde{Z}'_N)$ is Gaussian with zero mean and covariance matrix $\mathbf{S} = \mathbf{R}^{-1}\mathbf{R}^{-T}$ (\mathbf{R} is invertible). Note that

$$I(\mathbf{X}; \tilde{\mathbf{Y}}') = h(\tilde{\mathbf{Y}}') - h(\tilde{\mathbf{Z}}') \leq \sum_{i=1}^N h(\tilde{Y}'_i) - h(\tilde{Z}'_i), \quad (21)$$

which follows using the chain rule and since conditioning reduces entropy. Adding $\sum_{i=1}^N (h(\tilde{Z}''_i) - h(\tilde{Z}'_i)) = 0$ to this upper bound, where \tilde{Z}''_i is $\mathcal{N}(0, s_{i,i})$, leads to

$$\sum_{i=1}^N (h(\tilde{Y}'_i) - h(\tilde{Z}'_i)) + \sum_{i=1}^N h(\tilde{Z}''_i) - h(\tilde{Z}'_i) \quad (22)$$

Note that $\sum_{i=1}^N h(\tilde{Z}''_i) - h(\tilde{Z}'_i) = \frac{1}{2} \log \left(\frac{\prod_{i=1}^N s_{i,i}}{|\mathbf{S}|} \right)$. Furthermore, $\sum_{i=1}^N (h(\tilde{Y}'_i) - h(\tilde{Z}'_i)) = \sum_{i=1}^N I(X_i; \tilde{Y}'_i)$. But

$$\max_{p(\mathbf{x})} \sum_{i=1}^N I(X_i; \tilde{Y}'_i) \leq \max_{\mathcal{E} \in \mathcal{S}} \sum_{i=1}^N \max_{\substack{p(x_i) \\ \mathbb{E}[X_i] \leq \mathcal{E}_i}} I(X_i; \tilde{Y}'_i). \quad (23)$$

The inner maximization is the capacity of the channel $\tilde{y}'_i = x_i + \tilde{z}'_i$ where $x_i \geq 0$ and $\mathbb{E}[X_i] \leq \mathcal{E}_i$, which is $c(s_{i,i}^{-\frac{1}{2}}, \mathcal{E}_i)$. This in turn is upper bounded by $\bar{r}(s_{i,i}^{-\frac{1}{2}}, \mathcal{E}_i)$ (8), which concludes the proof. ■

Next, we compare this upper bound and the lower bounds in Prop. 1–3.

VI. COMPARISON

In Fig. 2, we plot the capacity upper bound $\bar{C}(\mathbf{H}, \mathcal{E})$ (Theorem 1) along with the achievable rates $R_m^{[I]}(\mathbf{H}, \mathcal{E})$ (Prop. 1), $R_m^{[QR]}(\mathbf{H}, \mathcal{E})$ (Prop. 2), and $R_m^{[SVD]}(\mathbf{H}, \mathcal{E})$ (Prop. 3), for the 4×4 MIMO channel given in [8, eq. (14)] corresponding to a transmitter with four light fixtures and a receiver with four detectors. The parameters of the transmit and receive apertures can be found in [8]. We plot the achievable rates versus SNR, defined as the ratio $\frac{\varepsilon}{\sigma}$ where σ^2 is the noise variance of each receiver, assumed here equal to one. The same intensity allocation used for continuous distributions (obtained similar to [18]) is used for the discrete ones.

We highlight some observations in this figure. First the rates achievable using the precoding free schemes (inversion and QR) are higher than those achievable using the DC-offset SVD based scheme. The performance gap between the two is as large as ≈ 3.6 dB at high SNR for this channel. This owes to the fact that under DC-offset operation, additional constraints have to be imposed on the channel inputs leading to loss in achievable rate. Second, QR decomposition is better than channel inversion, which is consistent with intuition since channel inversion amplifies noise contrary to QR decomposition. Finally, we see that the lower bounds achieved using inversion or QR decomposition and the upper bound are close at high SNR, with the achievable rate of QR decomposition being closer than that of channel inversion. It can be further proved that QR decomposition is optimal at high-SNR as shown next.

Theorem 2: For a MIMO IM-DD channel with an invertible channel matrix \mathbf{H} , the capacity satisfies

$$\lim_{\mathcal{E} \rightarrow \infty} \left[C(\mathbf{H}, \mathcal{E}) - R_e^{[QR]}(\mathbf{H}, \mathcal{E}) \right] = 0. \quad (24)$$

Furthermore, for large \mathcal{E} , $C(\mathbf{H}, \mathcal{E}) \approx \frac{1}{2} \log \left[\frac{e\mathcal{E}^2}{2\pi N^2} \mathbf{H}\mathbf{H}^T \right]$.

Proof: We start with the upper bound $\bar{C}(\mathbf{H}, \mathcal{E})$ in Theorem 1. From [15], we have that $\bar{r}(s_{i,i}^{-\frac{1}{2}}, \mathcal{E}_i)$ converges to $\frac{1}{2} \log \left(\frac{e\mathcal{E}_i^2}{2\pi s_{i,i}} \right)$ as \mathcal{E}_i grows. Furthermore, we have from [18] that the solution of $\max_{\mathcal{E} \in \mathcal{S}} \sum_{i=1}^N \bar{r}(s_{i,i}^{-\frac{1}{2}}, \mathcal{E}_i)$ for large \mathcal{E} is $\mathcal{E}_i = \frac{\mathcal{E}}{N}$. Therefore, as \mathcal{E} grows, $\max_{\mathcal{E} \in \mathcal{S}} \sum_{i=1}^N \bar{r}(s_{i,i}^{-\frac{1}{2}}, \mathcal{E}_i)$ converges to $\sum_{i=1}^N \frac{1}{2} \log \left(\frac{e\mathcal{E}^2}{2\pi s_{i,i} N^2} \right)$ and the upper bound $\bar{C}(\mathbf{H}, \mathcal{E})$ converges to $\sum_{i=1}^N \frac{1}{2} \log \left(\frac{e\mathcal{E}^2}{2\pi N^2} \right) - \frac{1}{2} \log |\mathbf{S}|$. Now $|\mathbf{S}| = |\mathbf{R}|^{-2} = \prod_{i=1}^N r_{i,i}^{-2}$ since \mathbf{R} is triangular. Thus, $\bar{C}(\mathbf{H}, \mathcal{E})$ converges to $\sum_{i=1}^N \frac{1}{2} \log \left(\frac{e r_{i,i}^2 \mathcal{E}^2}{2\pi N^2} \right)$ as \mathcal{E} grows. But $R_e^{[QR]}(\mathbf{H}, \mathcal{E}) \geq \sum_{i=1}^N \frac{1}{2} \log \left(\frac{e r_{i,i}^2 \mathcal{E}^2}{2\pi N^2} \right)$ since $\mathcal{E}_i = \mathcal{E}/N$ is a valid intensity allocation. Thus, the achievable rate using QR-decomposition, exponentially distributed inputs, and equal intensity allocation coincides with the upper bound at high SNR, which proves the first statement. The second statement follows since $\prod_{i=1}^N r_{i,i}^2 = |\mathbf{H}\mathbf{H}^T|$. ■

The geometric distribution is also optimal in conjunction with QR decomposition at high SNR.

The high-SNR gap between QR and channel inversion can be computed as follows. In channel inversion, the high-SNR achievable rate $R_e^{[I]}(\mathbf{H}, \mathcal{E})$ (similar discussion holds for $R_g^{[I]}(\mathbf{H}, \mathcal{E})$) converges to $\max_{\mathcal{E} \in \mathcal{S}} \sum_{i=1}^N \frac{1}{2} \log \left(\frac{e\mathcal{E}_i^2}{2\pi \|\mathbf{u}_i\|^2} \right)$, where the maximization is achieved by $\mathcal{E}_i = \frac{\mathcal{E}}{N}$ [18]. Thus, the achievable rate at high SNR satisfies

$$\lim_{\mathcal{E} \rightarrow \infty} \left[R_e^{[I]}(\mathbf{H}, \mathcal{E}) - \sum_{i=1}^N \frac{1}{2} \log \left(\frac{e\mathcal{E}^2}{2\pi \|\mathbf{u}_i\|^2 N^2} \right) \right] = 0.$$

Therefore, the high-SNR gap between QR and inversion is

$$\Delta = \sum_{i=1}^N \frac{1}{2} \log (r_{i,i}^2 \|\mathbf{u}_i\|^2). \quad (25)$$

Using simple manipulations, it can be shown that this gap implies that inversion requires $\Delta_{dB} = 10 \log_{10} \left(\sqrt{N} \prod_{i=1}^N |r_{i,i}| \|\mathbf{u}_i\| \right)$ extra dBs (in \mathcal{E}/σ) to achieve the same rate as QR, at high SNR. In this exemplary channel, the gap is ≈ 0.9 dB.

This gap is always positive. To see this, note that $\prod_{i=1}^N r_{i,i}^2 = |\mathbf{H}\mathbf{H}^T|$ and that $\prod_{i=1}^N \|\mathbf{u}_i\|^2 \geq |\mathbf{H}^{-1}\mathbf{H}^{-T}|$ by Hadamard's inequality, with equality if and only if $\mathbf{H}^{-1}\mathbf{H}^{-T}$ is diagonal. Thus, $\Delta \geq 0$. Note that $\mathbf{H}^{-1}\mathbf{H}^{-T}$ is diagonal if and only if $\mathbf{H}^T\mathbf{H}$ is diagonal, which means \mathbf{H} has orthogonal columns. Since $h_{i,j} \geq 0$, \mathbf{H} has orthogonal columns if and only if it is diagonal, for which the MIMO channel reduces to a system of parallel channels, see [18].

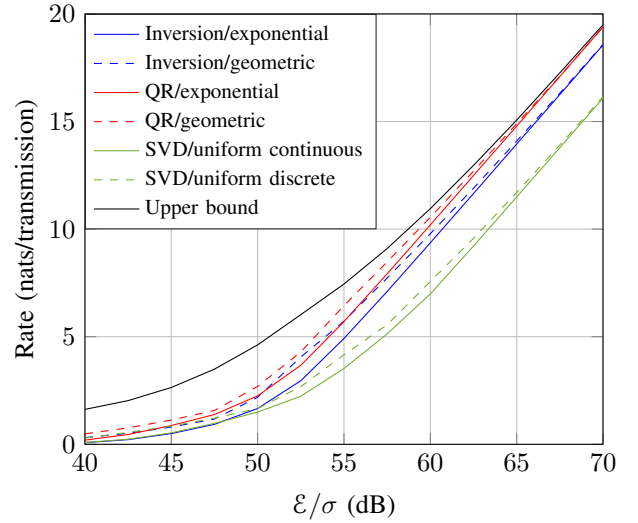


Fig. 2: Achievable rates and upper bounds for the MIMO channel in [8, eq. (14)].

Similarly, the high SNR gap between $R_e^{[QR]}(\mathbf{H}, \mathcal{E})$ and $R_u^{[SVD]}(\mathbf{H}, \mathcal{E})$ can be shown to be

$$\Delta' = \frac{N}{2} \log \left(\frac{e^2}{4} \right) + \frac{1}{2} \log \left(\frac{\prod_{i=1}^N r_{i,i}^2}{\prod_{i=1}^N \nu_i^2} \right). \quad (26)$$

This gap is equivalent to $\Delta'_{dB} = 10 \log_{10} \left(\frac{e}{2} \sqrt{N} \sqrt{\frac{\prod_{i=1}^N r_{i,i}}{\prod_{i=1}^N \nu_i}} \right)$ dB. In this exemplary channel, the gap is ≈ 3.6 dB. Similar to Δ , Δ' is the smallest when the MIMO channel \mathbf{H} has a diagonal structure, i.e., a system of parallel channels. To see this, note that $\prod_{i=1}^N r_{i,i}^2 = |\mathbf{H}\mathbf{H}^T| = \prod_{i=1}^N \sigma_i^2$. Note also that $\nu_i^2 = \left(\sum_{j=1}^N |v_{j,i}| \right)^2 \geq \sum_{j=1}^N v_{j,i}^2 = 1$ since \mathbf{V} is an orthogonal matrix. Therefore, the smallest gap Δ' is $\frac{N}{2} \log \left(\frac{e^2}{4} \right)$ which occurs when \mathbf{V} is equal to the identity matrix. But this implies that $\mathbf{H} = \mathbf{U}\mathbf{\Sigma}$ has orthogonal columns, and since \mathbf{H} has positive components, this can only be the case if \mathbf{H} is diagonal.

It is also interesting to compare the schemes in terms of their CSI requirements at the transmitter. Both inversion and QR schemes are superior in this aspect in comparison with the DC-offset SVD scheme. The achievability of $R_m^{[I]}(\mathbf{H}, \mathcal{E})$ in Prop. 1 requires the feedback of N variables ($\|\mathbf{u}_i\|$, $i = 1, \dots, N$) required for intensity allocation. Similarly, the achievability of $R_m^{[QR]}(\mathbf{H}, \mathcal{E})$ in Prop. 2 requires the feedback of N variables ($|r_{i,i}|$, $i = 1, \dots, N$). Moreover, at high SNR, no CSI feedback is required because equal intensity allocation is optimal in this regime [18]. However, the achievability of $R_m^{[SVD]}(\mathbf{H}, \mathcal{E})$ requires the feedback of N^2 variables since it requires the knowledge of \mathbf{H} at the transmitter (or at least $\mathbf{\Sigma}\mathbf{V}^T$).

Suppose channel state information is not available at the transmitter. In this case, the DC-offset SVD scheme fails, while the channel inversion and the QR schemes can still be used. As an example, consider a MIMO channel which follows a *log-normal fading* (weak turbulence [1]) with Rytov variance 1. Suppose that due to the absence of CSI, we constrain the

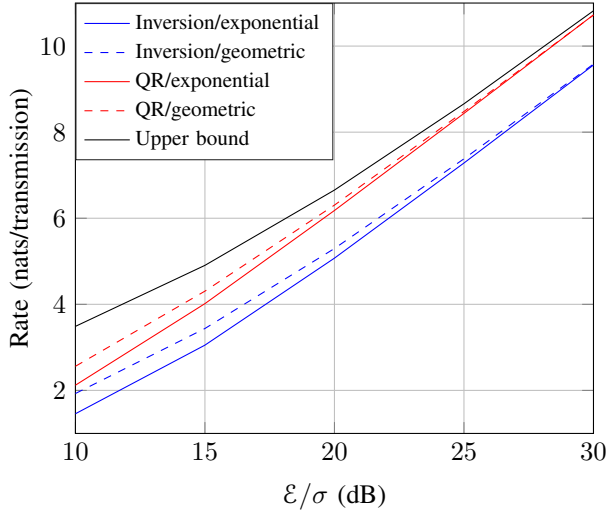


Fig. 3: Ergodic rates for a MIMO channel with $N = 2$ under log-normal fading.

transmitter to allocate the intensity \mathcal{E} equally across the N apertures. Under this condition, the ergodic achievable rate using channel inversion becomes

$$R_{m,\text{erg}}^{[I]}(\mathcal{E}) = \mathbb{E}_{\mathbf{H}} \left[\sum_{i=1}^N r_m \left(\|\mathbf{u}_i\|^{-1}, \frac{\mathcal{E}}{N} \right) \right], \quad m \in \{\mathbf{e}, \mathbf{g}\}, \quad (27)$$

where \mathbf{u}_i^T is as defined in Prop. 1. Similarly, the ergodic achievable rate using QR-decomposition becomes

$$R_{m,\text{erg}}^{[QR]}(\mathcal{E}) = \mathbb{E}_{\mathbf{H}} \left[\sum_{i=1}^N r_m \left(|r_{i,i}|, \frac{\mathcal{E}}{N} \right) \right], \quad m \in \{\mathbf{e}, \mathbf{g}\}, \quad (28)$$

where $r_{i,i}$ is as defined in Prop. 2. An upper bound on the ergodic capacity is given by

$$\bar{C}_{\text{erg}}(\mathcal{E}) = \mathbb{E}_{\mathbf{H}} \left[\sum_{i=1}^N \bar{r} \left(s_{i,i}^{-\frac{1}{2}}, \frac{\mathcal{E}}{N} \right) + \frac{1}{2} \log \left(\frac{\prod_{i=1}^N s_{i,i}}{|\mathbf{S}|} \right) \right], \quad (29)$$

with $s_{i,i}$ and \mathbf{S} as defined in Theorem 1. Fig. 3 shows these ergodic rates versus SNR under log-normal fading for a MIMO channel with $N = 2$. Note the high-SNR optimality of the QR-decomposition based scheme, and the sub-optimality of the channel inversion based scheme. The high SNR gap between the two is ≈ 2.5 dB.

VII. CONCLUSION

We studied several MIMO schemes for IM-DD systems in terms of their achievable rates. The SVD-based precoding/postcoding scheme - which is optimal in RF MIMO - must be modified to a DC-offset SVD-based scheme in IM-DD MIMO, leading to a sub-optimal performance. To avoid this deterioration, precoding free schemes are favored in IM-DD MIMO. We have derived achievable rates of channel inversion and QR-decomposition based schemes. Such schemes outperform the SVD-based scheme. Furthermore, we have shown that the QR-based scheme is optimal at high SNR, thus characterizing the channel's high-SNR capacity. An advantage

of precoding free schemes is their lower requirement of CSI at the transmitter compared with the SVD-based scheme, although some CSI is still required at the transmitter to perform intensity allocation. If intensity allocation is not permitted, then precoding free schemes do not need any CSI at the transmitter, and the QR-based scheme achieves the high-SNR ergodic capacity of the channel, which is demonstrated numerically under log-normal fading.

REFERENCES

- [1] M. A. Khalighi and M. Uysal, "Survey on free space optical communications: A communication theory perspective," *IEEE Communication Surveys and Tutorials*, vol. 16, no. 4, pp. 2231–2258, 4th quarter 2014.
- [2] H. Burchardt, N. Serafimovski, D. Tsonev, S. Videv, and H. Haas, "VLC: Beyond point-to-point communication," *IEEE Communications Magazine*, vol. 52, no. 7, pp. 98–105, July 2014.
- [3] M. Khalighi, N. Schwartz, N. Aitamer, and S. Bourennane, "Fading reduction by aperture averaging and spatial diversity in optical wireless systems," *IEEE/OSA Journal of Optical Communications and Networking*, vol. 1, no. 6, pp. 580–593, November 2009.
- [4] N. Letzepis and A. Guillen i Fàbregas, "Outage probability of the Gaussian MIMO free-space optical channel with PPM," *IEEE Transactions on Communications*, vol. 57, no. 12, pp. 3682–3690, December 2009.
- [5] D. Bushuev and S. Arnon, "Analysis of the performance of a wireless optical multi-input to multi-output communication system," *Journal of the Optical Society of America. A, Optics, Image Science, and Vision*, vol. 23, no. 7, pp. 1722–1730, July 2006.
- [6] G. Yang, M.-A. Khalighi, T. Virieux, S. Bourennane, and Z. Ghassemloo, "Contrasting space-time schemes for MIMO FSO systems with non-coherent modulation," in *International Workshop on Optical Wireless Communications (IWOW)*, Oct 2012, pp. 1–3.
- [7] L. Zeng, D. O'Brien, H. Minh, G. Faulkner, K. Lee, D. Jung, Y. Oh, and E. T. Woon, "High data rate multiple input multiple output (MIMO) optical wireless communications using white LED lighting," *IEEE Journal on Selected Areas in Communications*, vol. 27, no. 9, pp. 1654–1662, December 2009.
- [8] T. Fath and H. Haas, "Performance comparison of MIMO techniques for optical wireless communications in indoor environments," *IEEE Transactions on Communications*, vol. 61, no. 2, pp. 733–742, February 2013.
- [9] S. M. Haas and J. H. Shapiro, "Capacity of the multiple-input, multiple-output poisson channel," in *Stochastic Theory and Control*, ser. Lecture Notes in Control and Information Sciences, B. Pasik-Duncan, Ed. Springer Berlin Heidelberg, 2002, vol. 280, pp. 155–168.
- [10] —, "Capacity of wireless optical communications," *IEEE Journal on Selected Areas in Communications*, vol. 21, no. 8, pp. 1346–1357, Oct 2003.
- [11] P. Butala, H. Elgala, and T. Little, "SVD-VLC: A novel capacity maximizing VLC MIMO system architecture under illumination constraints," in *IEEE Globecom Workshops*, Dec 2013, pp. 1087–1092.
- [12] K. H. Park, Y. C. Ko, and M. S. Alouini, "On the power and offset allocation for rate adaptation of spatial multiplexing in optical wireless MIMO channels," *IEEE Transactions on Communications*, vol. 61, no. 4, pp. 1535–1543, April 2013.
- [13] M. Arar and A. Yongacoglu, "Efficient detection algorithm for 2Nx2N MIMO systems using alamouti code and QR decomposition," *IEEE Communications Letters*, vol. 10, no. 12, pp. 819–821, December 2006.
- [14] E. Monteiro and S. Hranilovic, "Design and implementation of color-shift keying for visible light communications," *Journal of Lightwave Technology*, vol. 32, no. 10, pp. 2053–2060, May 2014.
- [15] A. Lapidoth, S. M. Moser, and M. Wigger, "On the capacity of free-space optical intensity channels," *IEEE Trans. on Info. Theory*, vol. 55, no. 10, pp. 4449–4461, Oct. 2009.
- [16] A. A. Farid and S. Hranilovic, "Capacity bounds for wireless optical intensity channels with Gaussian noise," *IEEE Trans. on Info. Theory*, vol. 56, no. 12, pp. 6066–6077, Dec. 2010.
- [17] A. Chaaban, J.-M. Morvan, and M.-S. Alouini, "Free-space optical communications: Capacity bounds, approximations, and a new sphere-packing perspective," *IEEE Trans. on Communications*, vol. 64, no. 3, pp. 1176–1191, March 2016.
- [18] A. Chaaban, Z. Rezk, and M.-S. Alouini, "Capacity bounds for parallel optical wireless channels," in *Proc. of IEEE International Conference on Communications (ICC)*, Kuala Lumpur, Malaysia, May 2016.